Guanine and nucleotide binding protein 3 promotes odonto/osteogenic differentiation of apical papilla stem cells via JNK and ERK signaling pathways

YANG ZHANG*, LICHAN YUAN*, LI MENG, MENGRU FANG, SHUYU GUO, DONGYUE WANG, JUNQING MA and LIN WANG

Jiangsu Key Laboratory of Oral Diseases, Nanjing Medical University, Nanjing, Jiangsu 210029, P.R. China

Received July 12, 2018; Accepted October 23, 2018

DOI: 10.3892/ijmm.2018.3984

Abstract. Odonto/osteogenic differentiation of stem cells from the apical papilla (SCAPs) is a key process in tooth root formation and development. However, the molecular mechanisms underlying this process remain largely unknown. In the present study, it was identified that guanine and nucleotide binding protein 3 (GNAI3) was at least in part responsible for the odonto/osteogenic differentiation of SCAPs. GNAI3 was markedly induced in mouse tooth root development *in vivo* and in human SCAPs mineralization *in vitro*. Notably, knockdown of GNAI3 by lentiviral vectors expressing short-hairpin RNAs against GNAI3 significantly inhibited the proliferation, cell cycle progression and migration of SCAPs, as well as odonto/osteogenic differentiation of SCAPs *in vitro*, suggesting that GNAI3 may play an essential role in tooth root development. The promotive role of GNAI3 in odonto/osteogenic differentiation was further confirmed by downregulation of odonto/osteogenic makers in GNAI3-deficient SCAPs. In addition, knockdown of GNAI3 effectively suppressed activity of c-Jun N-terminal kinase (JNK) and extracellular-signal regulated kinase (ERK) signaling pathways that was induced during SCAPs differentiation, suggesting that GNAI3 promotes SCAPs mineralization at least partially via JNK/ERK signaling. Taken together, the present results implicate GNAI3 as a critical regulator of odonto/osteogenic differentiation of SCAPs in tooth root development, and suggest a possible role of GNAI3 in regeneration processes in dentin or other tissues.

Correspondence to: Professor Lin Wang or Professor Junqing Ma, Jiangsu Key Laboratory of Oral Diseases, Nanjing Medical University, Building 2, 140 Han Zhong Road, Nanjing, Jiangsu 210029, P.R. China
E-mail: lw603@njmu.edu.cn
E-mail: jma@njmu.edu.cn

*Contributed equally

Key words: guanine and nucleotide binding protein 3, odonto/osteogenic differentiation, mitogen-activated protein kinase, apical papilla stem cells, tooth root formation

Introduction

Mesenchymal stem cells (MSCs) have been widely used for cell-based treatment of various diseases due to their immunomodulatory and anti-inflammatory properties (1). As a type of multipotent cell originating from bone marrow, MSCs can differentiate into various cell types including osteoblast, chondrocyte, myocyte and adipocyte cells (2-5). Dental stem cells are MSC-like cells isolated from dental tissues, and are classified into stem cells from the apical papilla (SCAPs), stem cells from human exfoliated deciduous teeth, periodontal ligament stem cells and dental pulp stem cells according to the subsites of dental tissues from which the cells are isolated (6-8). Dental tissues including wisdom and primary teeth are a reservoir of MSCs, contributing to the regeneration of dental tissues (9). Thus, MSCs are considered as a promising source in the context of regenerative medicine (10-13). Among the MSC types, SCAPs are present in the root apex of developing teeth, where they are considered to be associated with root development (14). SCAPs can be readily isolated from extracted wisdom teeth that are generally considered useless (15). In response to inflammatory stimuli, SCAPs have been identified to exhibit increased osteogenic and angiogenesis potential due to enhanced vitality and stemness (16).

Guanine nucleotide binding proteins (G proteins) are a family of regulatory proteins responsible for molecular signal transduction of extracellular signals to the intracellular environment (17). G proteins are typically composed of α, β and γ subunits. Gα subunits are categorized into 4 major classes based on sequence similarity and function of the α-subunit, termed Gαs, Gαi/o, Gαq/11 and Gα12/13 (18). The guanine nucleotide binding protein 3 (GNAI3) belongs to the Gαi subunit class and is located on chromosome 17q22-24 (19). Increasing evidence has demonstrated that GNAI3 is involved in a variety of cellular processes including proliferation, apoptosis and differentiation (19-22). GNAI3 has also been reported to regulate craniofacial growth and development, and homeotic modifications in the human GNAI3 gene may

lead to auriculo-condylar syndrome (ACS), an uncommon craniofacial natal defect characterized by mandible hypoplasia (23).

Mitogen-activated protein kinase (MAPK) has three major subfamilies, extracellular-signal regulated kinases (ERKs), c-Jun N-terminal kinases (JNKs) and p38 MAPKs. MAPK signaling serves an essential role in regulating cell proliferation and differentiation, and accumulating experimental data have demonstrated that MAPK is associated with osteogenic differentiation (24,25). Furthermore, bioinformatic analysis has identified that MAPK signaling pathways may play an important role in the SCAPs niche (26).

A previous study by our group demonstrated that GATA binding protein 4 (GATA4) regulated root development via GNAI3 (27). However, to our knowledge the role and mechanism of GNAI3 remain unknown. In the present study, the role of GNAI3 in regulating the proliferation, cell cycle progression, apoptosis, migration and odonto/osteogenic differentiation of SCAPs was investigated using loss-of-function assays. The molecular mechanism underlying the function of GNAI3 was also examined.

Materials and methods

Animals and histological analysis. A total of 20, 14 day-old male mice (C57BL/6J; weight 5.2-8.7g) were provided by the Animal Center of Nanjing Medical University (Nanjing, China) and maintained in a temperature-controlled room (room temperature 24±1˚C; relative humidity 50±10%; 12-h light/dark cycle; free access to mouse chow and water). The maxillary halves of the mice were isolated, fixed in 4% buffered formalin for 24 h at 4˚C, decalcified in 10% EDTA (pH 7.4) for 7 days at room temperature, paraffin-embedded and sectioned into 5-μm slices. Ethical approval for the animal experimentation was provided by the Experimental Animal Care and Use Committee of Nanjing Medical University (approval no. 2015-03-40).

The tissue sections were treated with 3% H_2O_2 for 30 min followed by normal goat serum (Wuhan Boster Biological Technology, Ltd., Wuhan, China) for 30 min at 37˚C, and subject to immunohistochemical staining for histological investigation. The sections were incubated with primary rabbit anti-mouse GNAI3 antibody (1:200 dilution; cat. no. ab154024) and primary monoclonal mouse anti-mouse nestin (1:100 dilution; cat. no. ab11306; both from Abcam, Cambridge, MA, USA) overnight at 4˚C. Nestin was used as a biomarker of mature and differentiated odontoblasts (28). Following three washes with 0.1 mol/l phosphate-buffered saline (PBS), the sections were incubated with secondary horseradish peroxidase (HRP)-conjugated antibody (KIT-5020; MaxVision Biosciences Inc., Fuzhou, China) for 30 min at 37˚C. The immunoreaction was localized using a diaminobenzidine kit (Beyotime Institute of Biotechnology, Haimen, China) according to the manufacturer's protocol and the sections were counterstained with hematoxylin for 5 min at 37˚C. Stained sections were observed and analyzed by ImageJ v.1.45 software (National Institutes of Health, Bethesda, NJ, USA) under a light microscope (DM4000; Leica Microsystems GmbH, Wetzlar, Germany) at x400 magnification.

Cell cultures and stem cell characterization. Between January and December 2017, a total of 20 male healthy patients (14-18 years of age) underwent extraction surgery at Stomatological Hospital of Jiangsu Province, Nanjing, China, and 20 wisdom teeth (one tooth per patient) with open apices were acquired. The use of human samples for the study was approved by the Medical Ethics Committee of Stomatological Hospital of Jiangsu Province (approval no. PJ2016-038-001). Consent was provided by the patients or their next of kin for the collection of the dental samples. Soft tissues of the root apex were collected immediately and washed with PBS. The separated apex tissues were minced with sterilized scissors and then digested with 3 mg/ml collagenase type I (Sigma Aldrich Chemie, Taufkirchen, Germany) and 4 mg/ml dispase (Roche Applied Science, Penzberg, Germany) for 1 h at 37˚C, and then the single cell suspensions were grown in α-minimum essential medium supplemented with 10% fetal bovine serum (FBS), 2 mmol/l glutamine, 100 U/ml penicillin and 100 mg/ml streptomycin (all from Invitrogen; Thermo Fisher Scientific, Inc., Waltham, MA, USA) in a humidified 5% CO_2 incubator at 37˚C. The culture medium was changed every 3 days. SCAPs at passage 2-5 were used in the subsequent experiments. To address the potential roles of JNK and ERK signaling pathways, specific JNK inhibitor (20 μM; SP600125), specific ERK inhibitor (20 μM; U0126; both from Beyotime Institute of Biotechnology) and dimethyl sulfoxide (20 μM; Sigma-Aldrich; Merck KGaA, Darmstadt, Germany) as a control were respectively added to the SCAPs, and the cells were incubated at 37˚C for 5 min (29,30). As for the characterization of cultured SCAPs, the cells were digested with trypsin (Roche Applied Science), collected and incubated with fluorochrome-conjugated rabbit anti-human antibodies: Cluster of differentiation (CD)90-fluorescein isothiocyanate (FITC; 561969), CD44-phycoerythrin (PE; 561858), CD45-allophycocyanin (560973) and CD14-PE-cyanine 7 (560919; all at 0.5 mg/ml; BD Biosciences, San Jose, CA, USA) for 1 h at 4˚C in the dark to detect the SCAPs phenotype (31,32). Following fixation with 4% paraformaldehyde buffer for 30 min at 4˚C, cells were washed twice with PBS containing 2% FBS (Hyclone; GE Healthcare Life Science, Logan, UT, USA) and stained cells were characterized and identified by flow cytometry (BD FACSCalibur™; BD Biosciences) (33). Data were analyzed with Summit 5.1 software (Beckman Coulter, Inc., Brea, CA, USA).

Lentiviral transduction. Recombinant lentiviral LV-3 [pGLVH1/green fluorescent protein (GFP)+Puro] vectors expressing GAIN3 short-hairpin RNAs (shGNAI3-GFP) were purchased from Shanghai GenePharma Co., Ltd. (Shanghai, China). The short-hairpin sequence was 5'-CCAGGGAAU AUCAGCUCAATT-3', and the sequence of 5'-TTCTCC GAACGTGTCACGT-3' was used as the negative control (shCTRL-GFP). When SCAPs were at 60-80% confluence, lentiviral particles were added to the medium with a multiplicity of infection of 30. The virus-containing medium was replaced with fresh normal medium after 24 h at 37˚C. The transduced cells (GFP-positive) were observed under a fluorescence microscope (DMI3000B; Leica Microsystems GmbH) at x100 magnification 72 h after transduction. GNAI3

inhibition efficiency was confirmed by western blotting and reverse transcription-quantitative polymerase chain reaction (RT-qPCR) assays.

Cell proliferation assay. The cell proliferation capacity of SCAPs following different treatments was evaluated by Cell Counting Kit-8 assay (CCK8; Dojindo Molecular Technologies, Inc., Kumamoto, Japan) according to the manufacturer's protocol. At 72 h after transduction of lentiviral vectors or exposure to inhibitors, the cells were seeded at a density of $1x10^3$ cells/well in 96-well plates. A total of 100 μl CCK8 solution was added on days 0, 1, 2, 3, 4, 5 and 6 days of cell plating, and the plates were incubated for 1 h at 37˚C. Cell number was assessed based on optical density (OD) measurements at 450 nm using a microplate reader. To assess cell cycle arrest, SCAPs transduced with lentiviral vectors or exposed to inhibitors were grown for 72 h, and then collected, washed with PBS and fixed overnight with 70% ethanol at 4˚C. Subsequently, the cells were washed and treated with RNase, then stained with 20 mg/ml propidium iodide (PI) for an additional 1 h at room temperature. Cell cycle distribution (populations in G1, G2, and S phases) was determined by flow cytometry (BD FACSverse™; BD Biosciences) and analyzed using FlowJo V7 software (Tree Star, Oregon, USA). For analysis of apoptosis, SCAPs were digested with 4 mg/ml trypsin and washed with ice-cold PBS at 72 h after transduction with shGNAI3-GFP or shCTRL-GFP. The SCAPs were then resuspended in ice-cold 0.1 mol/l PBS and stained with an Annexin V-FITC/PI kit (Nanjing KeyGen Biotech Co., Ltd., Nanjing, China) for 15 min in the dark at room temperature, according to the manufacturer's instructions. The apoptotic rates of the SCAPs were determined by flow cytometry (BD FACSverse™) and analyzed with FlowJo V7.

Cell migration assay. The cell migration capacity of SCAPs following different treatments was evaluated by a scratch wound healing assay. Cultured cells in 6-well plates at 80% confluence were mechanically wounded with a 200 μl sterile pipette tip. Cell debris was removed gently and the remaining cells were incubated with normal media. After 0, 12 and 24 h of incubation, photographs were taken under a light microscope (DMIL LED; Leica Microsystems GmbH) at x100. Cell migration rate was quantified by counting the migrating cells.

Alkaline phosphatase (ALP) activity assay. ALP activity was evaluated using a BCIP/NBT Alkaline Phosphatase Color Development kit (Beyotime Institute of Biotechnology) according to the manufacturer's protocol. SCAPs transduced with shGNAI3-GFP or shCTRL-GFP after 72 h were seeded at a density of $1x10^5$ cells/well in 6-well plates and cultured in mineralization-inducing media containing α-minimum essential medium (Gibco; Thermo Fisher Scientific, Inc.), 10% FBS (Hyclone; GE Healthcare Life Science), 100 U/ml penicillin, 100 μg/ml streptomycin, 100 μM ascorbic acid, 2 mM 2-glycerophosphate and 10 nm dexamethasone for 5 days at 37˚C. Images were captured using a light microscope (DMIL LED) at x100 magnification. The staining intensity was determined using ImageJ v.1.45 software (National Institutes of Health, Bethesda, NJ, USA).

Matrix mineralization assay. Alizarin red S (ARS) staining was performed to assess extracellular matrix mineralization. SCAPs transduced with shGNAI3-GFP or shCTRL-GFP after 72 h were seeded at a density of $1x10^5$ cells/well in 6-well plates and cultured in mineralization-inducing media for 2 weeks at 37˚C, followed by fixation with 75% ethanol for 30 min at room temperature. A 2% ARS solution was used for detection of calcium deposits. Images were captured using a light microscope (DMIL LED) at x100 magnification. The OD of ARS staining was measured using a microplate reader at 560 nm.

Western blot analysis. SCAPs following the indicated treatments were harvested and lysed in radioimmunoprecipitation assay buffer (Beyotime Institute of Biotechnology) containing 1 mM phenylmethylsulfonyl fluoride for 30 min at 4˚C. Cell debris was eliminated by centrifugation at 240 x g for 15 min at 4˚C and protein concentration was determined by the bicinchoninic acid method. A total of 30 μg protein per lane was loaded on 10% sodium dodecyl sulfate-polyacrylamide gels for electrophoresis, and then transferred to polyvinylidene fluoride membranes followed by blocking in 5% nonfat milk in tris-buffered saline/Tween-20. The membranes were incubated with primary antibodies overnight at 4˚C, then with secondary antibodies for 1 h at room temperature. The protein bands were visualized with electrochemiluminescence substrate solution (GE Healthcare Life Sciences, Little Chalfont, UK), and images were captured using a Micro Chemiluminescence system 4.2 (DNR Bio-Imaging Systems, Ltd., Jerusalem, Israel). Semi-quantitative analysis were performed using ImageJ v.1.45 software.

Protein expression of dentin sialophosphoprotein (DSPP), runt-related transcription factor 2 (RUNX2), osterix (OSX), osteopontin (OPN), osteocalcin (OCN) and bone morphogenetic protein 4 (BMP4), as established osteogenic and odontogenic markers (34-38), was determined. Activity of MAPK and JNK signaling was also assessed based on phosphorylation levels. The primary antibodies used were as follows: Rabbit anti-GNAI3 (1:1,000 dilution; cat. no. ab154024; Abcam), mouse anti-DSPP (1:1,000 dilution; cat. no. sc73632; Santa Cruz Biotechnology, Inc., Dallas, TX, USA), mouse anti- RUNX2 (1:1000; dilution; cat. no. ab76956), polyclonal rabbit anti-OSX (1:1,000 dilution; cat. no. ab22552), rabbit anti-OPN (1:1,000 dilution; cat. no. ab63856), polyclonal rabbit anti-OCN (1:1,000 dilution; cat. no. ab93876), rabbit anti-BMP4; 1:1,000 dilution; cat. no. ab39973; all from Abcam), rabbit anti-GAPDH (1:1,000 dilution; cat. no. AP0063; Bioworld Technology, Inc., St. Louis Park, MN, USA), anti-phosphorylated (p)-JNK (dilution 1:1,000; cat. no. 4668), anti-JNK (dilution 1:1,000; cat. no. 9252), anti-p-p38 (dilution 1:1,000; cat. no. 9211), anti-p38 (dilution 1:1,000; cat. no. 9212), anti-p-ERK (dilution 1:1,000; cat. no. 4370) and anti-ERK (dilution 1:1,000; cat. no. 4694; all from Cell Signaling Technology, Inc., Danvers, MA, USA). HRP-conjugated secondary antibodies were used prior to detection (1:8,000 dilution; cat. no. ZB-2301; Origene Technologies, Beijing, China) for 1 h at room temperature. Band densities were quantified relative to that of GADPH.

RT-qPCR. RNA expression of the osteogenic and odontogenic gene markers dentin matrix acidic phosphoprotein 1

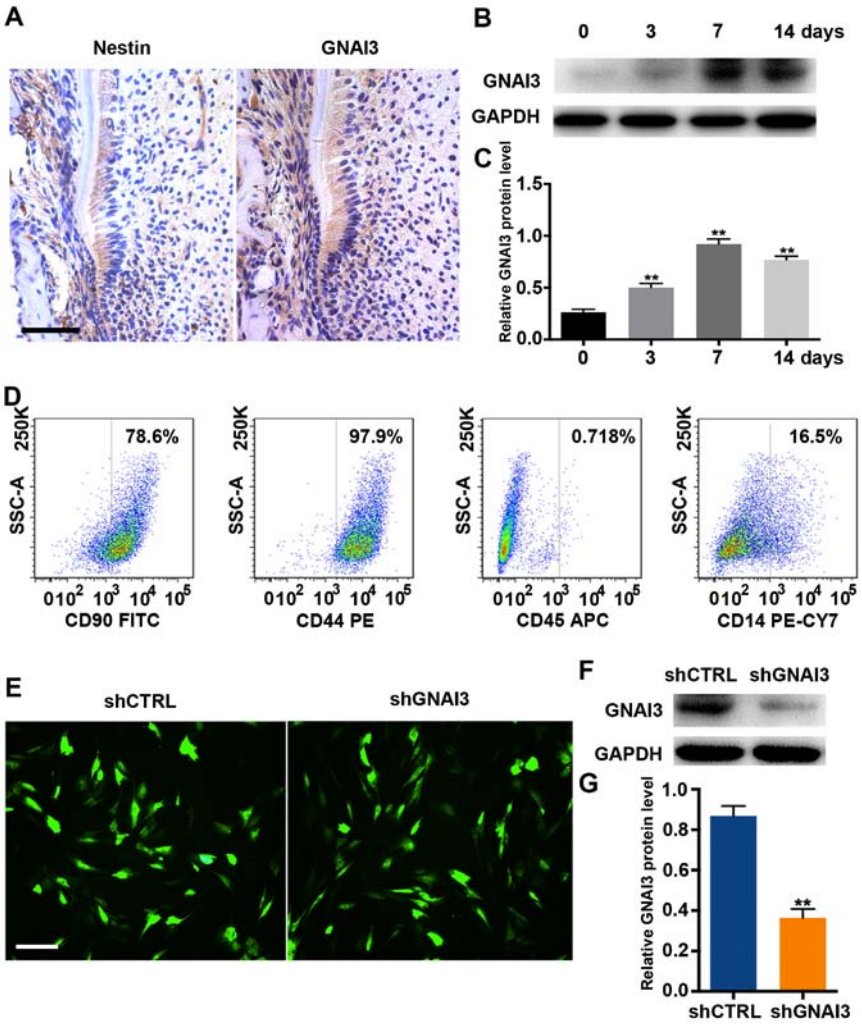

Figure 1. Upregulation of GNAI3 in mouse tooth root development *in vivo* and in human SCAPs mineralization *in vitro*. (A) Immunohistochemical staining for nestin (a biomarker of differentiated odontoblasts) and GNAI3 in mouse tooth roots on postnatal day 14. (B) Western blot analysis of GNAI3 expression in SCAPs following mineralization induction for the times indicated. (C) Quantification of western blot results in (B) by normalization to GAPDH. (D) Characterization of isolated human SCAPs by flow cytometry. (E) Detection of transduction efficiency of lentiviral particles expressing shRNA (multiplicity of infection of 30) in human SCAPs. After 3 days of transduction, GFP fluorescence was observed under a fluorescence microscope. (F) Western blot analysis of GNAI3 expression in SCAPs transduced with shGNAI3-GFP or shCTRL-GFP. (G) Quantification of western blot results in (F) by normalization to GAPDH. Scale bars: (A) 100 μm; (E) 400 μm. **P<0.01 vs. (B) day 0 group or (G) shCTRL group. GNAI3, guanine and nucleotide binding protein 3; SCAPs, stem cells of the apical papilla; sh[RNA], short hairpin [RNA]; GFP, green fluorescent protein; CTRL, control; CD, cluster of differentiation; FITC, fluorescein isothiocyanate; PE, phycoerythrin; APC, allophycocyanin; CY7, cyanine 7.

(DMP1), DSPP, OCN, OPN, OSX and RUNX2 (39) was determined. Total RNA was extracted from SCAPs using an RNApure High-purity Total RNA Rapid Extraction kit (Invitrogen; Thermo Fisher Scientific, Inc.) and then reverse transcribed into complementary DNA using a PrimeScript RT reagent kit (Takara Bio, Inc., Otsu, Japan) according to the manufacturer's protocol. The qPCR reactions were performed using a SYBR-Green RT-qPCR kit (Vazyme, Piscataway, NJ, USA) in 96-wells plates according to the manufacturer's protocol on a 7300 Real-Time PCR System (Applied Biosystems; Thermo Fisher Scientific, Inc.). Each 20-μl qPCR reaction system contained 10 μl SYBR-Green qPCR Master Mix, 2 μl cDNA and 0.4 μl of each primer (final primer concentration of 0.2 μM). The amplifications were performed under the following conditions: 95˚C for 30 sec, followed by 40 cycles of 95˚C for 10 sec, 60˚C for 30 sec, 95˚C for 15 sec, 60˚C for 1 min and 95˚C for 15 sec. GAPDH was used as the internal control. The primer sequences were as follows: GNAI3 forward, 5'-GGGAAG ACAAATGAAAGAGAA-3' and reverse, 5'-CCAACAAAG GCACTGAAC-3'; DMP1 forward, 5'-GGAAGAGGTGGT GAGTGAG-3' and reverse, 5'-TTGAGTGGGAGAGTGTG TG-3'; DSPP forward, 5'-CCATTCCAGTTCCTCAAA-3' and reverse, 5'-GCCTTCCTCTATCACCTTC-3'; OCN forward, 5'-CACACTCCTCGCCCTATT-3' and reverse, 5'-GGTCTCTTCACTACCTCGCT-3'; OPN forward, 5'-CTC CAATCGTCCCTACAGTCG-3' and reverse, 5'-CCAAGC TATCACCTCGGCC-3'; OSX forward, 5'-CTACCCATC TGACTTTGCTC-3' and reverse, 5'-CACTATTTCCCA CTGCCTT-3'; RUNX2 forward, 5'-AGTTCCCAAGCA TTTCATC-3' and reverse, 5'-GGCAGGTAGGTGTGG TAGT-3'; and GAPDH forward, 5'-TGAACCATGAGAAGT ATGACAACA-3' and reverse, 5'-TCTTCTGGGTGG CAGTG-3'. RT-qPCR for each sample was performed in triplicate and repeated three times. The relative expression of target mRNAs was determined using the $2^{-\Delta\Delta Cq}$ method (40).

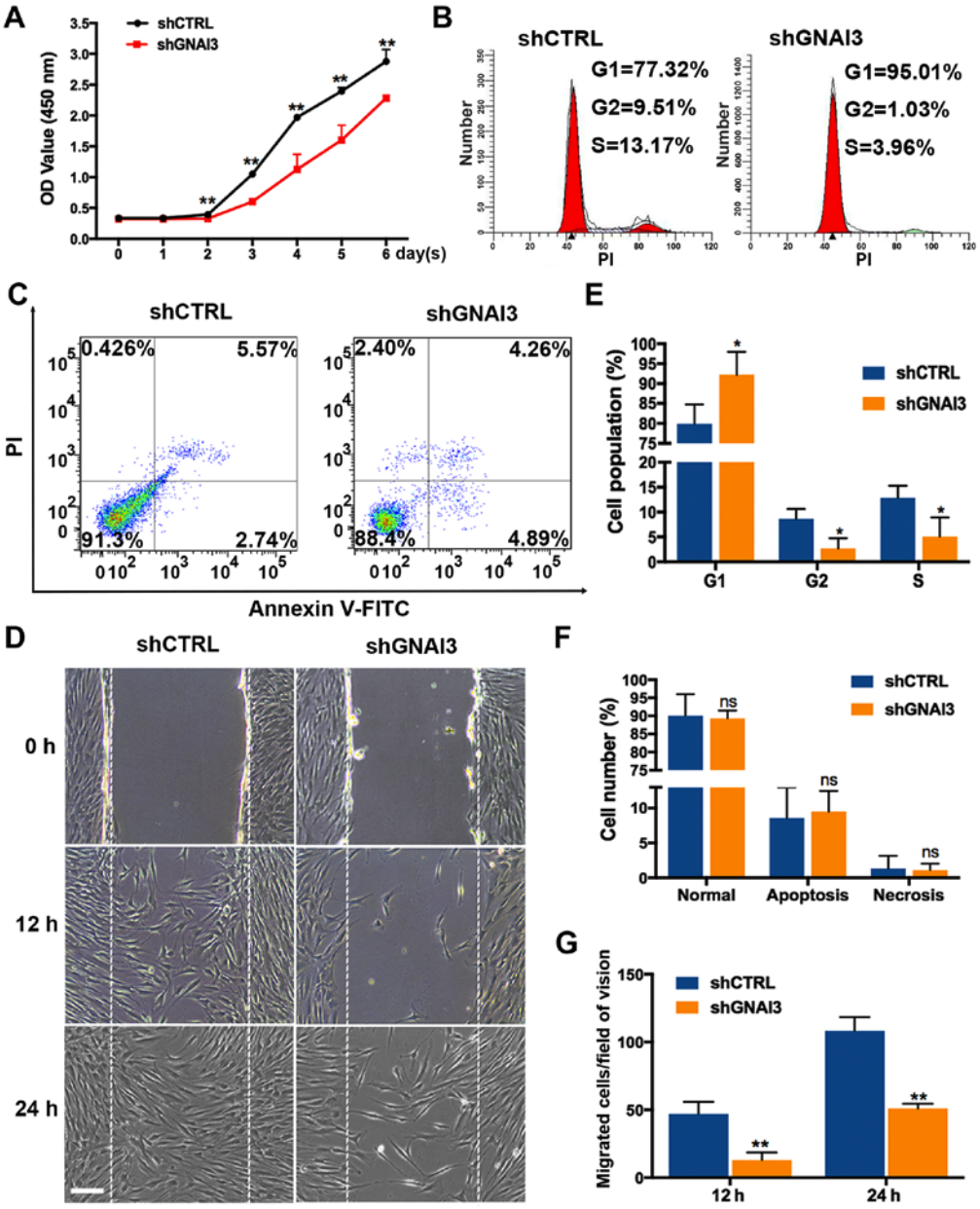

Figure 2. (A-G) Effect of GNAI3 knockdown on the proliferation and migration of SCAPs. (A) Cell Counting Kit-8 assay of the time course of SCAPs proliferation. (B and E) Flow cytometry assay of cell cycle progression in SCAPs. (C and F) Flow cytometry assay of SCAPs apoptosis and necrosis. (D) Scratch wound healing assay of SCAPs migration rates at 12 and 24 h of mineralization induction. (G) Quantification of SCAPs migration rates in (D). Scale bar: 200 μm. *P<0.05 and **P<0.01 vs. corresponding shCTRL group. GNAI3, guanine and nucleotide binding protein 3; SCAPs, stem cells of the apical papilla; sh[RNA], short hairpin [RNA]; CTRL, control; OD, optical density; PI, propidium iodide; FITC, fluorescein isothiocyanate.

Statistical analysis. Data are expressed as the mean ± standard deviation and were analyzed using SPSS 13 software (SPSS, Inc., Chicago, IL USA). The column graphs and line charts were generated using GraphPad Prism 7 (GraphPad, Inc., La Jolla, CA, USA). Independent two-sample t-tests were applied to compare the differences between the experimental and control groups. P<0.05 was considered to indicate a statistically significant difference.

Results

GNAI3 is induced in tooth root development in vivo and in SCAP mineralization in vitro. To determine the role of GNAI3 in tooth root development (dentin mineralization), the expression pattern of GNAI3 during root development and dentin mineralization was first examined. As depicted in Fig. 1A, GNAI3 was primarily expressed in Hertwig's epithelial root sheath (HERS) and the surrounding mesenchyme in mice, suggesting the possible involvement of GNAI3 in tooth root development. In addition, it was identified that GNAI3 expression was significantly upregulated in human SCAPs as early as 3 days after mineralization induction, with a peak at 7 days of induction (P<0.01; Fig. 1B and C). These results suggested that GNAI3 may be involved in tooth root development *in vivo* and *in vitro*.

To further investigate whether GNAI3 plays a role in mineralization induction of human SCAPs that were defined as CD90+/CD44+/CD45-/CD14- (Fig. 1D), lentiviral vector

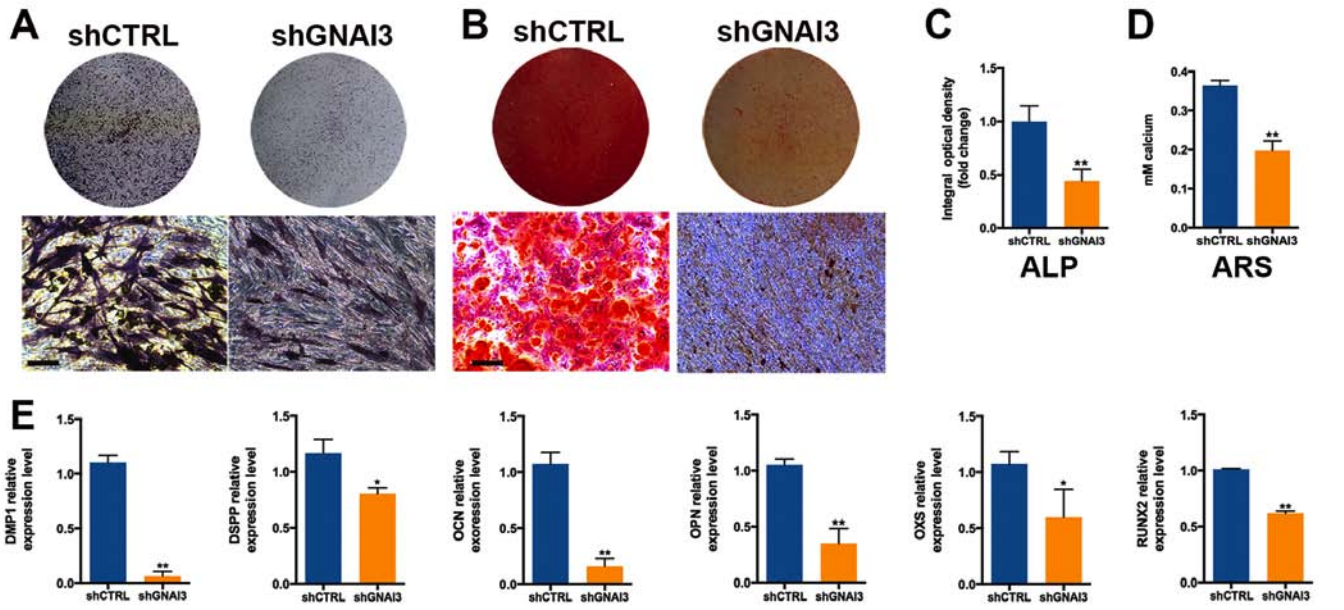

Figure 3. Effect of GNAI3 knockdown on the odonto/osteogenic differentiation of SCAPs. (A) ALP staining assay of SCAPs mineralization. (B) ARS staining assay for the accumulation of calcium during SCAPs mineralization. (C) Quantification of ALP staining in (A). (D) Quantification of ARS staining in (B). (E) Quantitative polymerase chain reaction detection of the mRNA expression of odonto/osteogenic markers as indicated. Scale bar: 200 μm. *P<0.05 and **P<0.01 vs. corresponding shCTRL group. GNAI3, guanine and nucleotide binding protein 3; SCAPs, stem cells of the apical papilla; sh[RNA], short hairpin [RNA]; CTRL, control; DMP1, dentin matrix acidic phosphoprotein 1; DSPP, dentin sialophosphoprotein; OCN, osteocalcin; OPN, osteopontin; OSX, osterix; RUNX2, runt-related transcription factor 2.

expressing shGNAI3 (shGNAI3-GFP) was used to knock down the expression of GNAI3. Lentiviral transduction efficiency (~90%) is shown in Fig. 1E. Importantly, shGNAI3-GFP effectively inhibited the expression of GNAI3 in SCAPs, compared with the control group (P<0.01; Fig. 1F and G), indicating that shGNAI3-GFP could be used for loss-of-function assays to detect the function of GNAI3 in SCAPs.

GNAI3 knockdown suppresses the proliferation and migration of SCAPs. It was subsequently determined whether GNAI3 regulates the proliferation and migration of SCAPs, two important processes in tooth root development. The results (Fig. 2) showed that GNAI3 knockdown by shGNAI3-GFP inhibited SCAPs growth over 2-6 days after transduction (P<0.01) in an apparent time-dependent manner (Fig. 2A), as well as cell cycle progression, as evidenced by G1 phase arrest (increased G1-phase cells) and decreased S and G2-phase populations of GNAI3-deficient SCAPs (P<0.05; Fig. 2B and E). However, GNAI3 knockdown had no apparent effect on the apoptosis or necrosis of SCAPs (Fig. 2C and F). In addition, GNAI3-deficient SCAPs exhibited markedly reduced migration ability 12 and 24 h after wounding, compared with control SCAPs (P<0.01; Fig. 2D and G). Collectively, these data indicated that GNAI3 is required for SCAPs proliferation and migration *in vitro*.

GNAI3 knockdown inhibits the odonto/osteogenic differentiation of SCAPs. Since dentin mineralization is a key event in tooth root development, the effects of GNAI3 knockdown on dentin mineralization resulting from odonto/osteogenic differentiation of SCAPs were investigated (Fig. 3). As displayed in Fig. 3A and C, GNAI3 knockdown significantly decreased ALP activity in SCAPs 5 days after mineralization induction (P<0.01). Consistently, GNAI3 knockdown significantly reduced ARS staining intensity 2 weeks after the mineralization induction of SCAPs (P<0.01; Fig. 3B and D). These results demonstrated that GNAI3 deficiency may increase calcium loss in SCAPs, suggesting an essential role of GNAI3 in the dentin mineralization and/or odonto/osteogenic differentiation of SCAPs.

To further confirm the function of GNAI3 in the odonto/osteogenic differentiation of SCAPs, the expression of odonto/osteogenic differentiation and mineralization markers was examined in GNAI3-deficient SCAPs. As shown in Fig. 3E, GNAI3-deficient SCAPs exhibited significantly decreased mRNA expression of the markers DMP1 (P<0.01), DSPP (P<0.05), OCN (P<0.01), OPN (P<0.01), OXS (P<0.05) and RUNX2 (P<0.01), compared with control SCAPs. Similar results were observed at the level of protein expression for the markers DSPP, RUNX2, OSX, OPN, OCN and BMP4 (all P<0.05 or <0.01; Fig. 4A and B). DMP1 protein expression was not detected as sufficient bands could not be obtained despite multiple attempts with different antibodies. Taken together, these data demonstrate that GNAI3 may be a critical regulator of odonto/osteogenic differentiation in SCAPs, suggesting a potential function in tooth root development.

GNAI3 knockdown inactivates JNK/ERK signaling pathways in the odonto/osteogenic differentiation of SCAPs. Subsequently, the molecular mechanisms underlying the function of GNAI3 in the odonto/osteogenic differentiation of SCAPs were investigated. SCAPs transfected with shGNAI3 or shCTRL lentivirus underwent osteogenic differentiation for 7 days before extracting total protein. It was observed that GNAI3 knockdown markedly downregulated the phosphorylation levels of JNK (P<0.01) and ERK

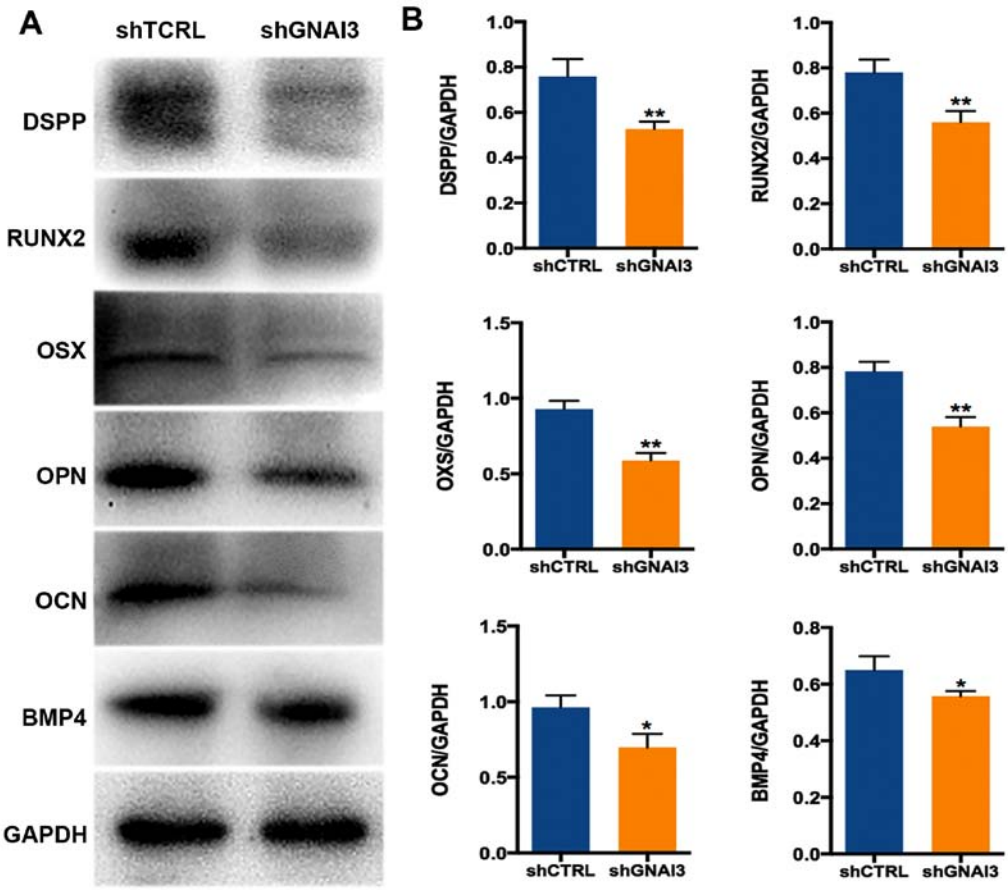

Figure 4. Effect of GNAI3 knockdown on the protein expression of odonto/osteogenic markers. Protein lysates of stem cells of the apical papilla transduced with shGNAI3-GFP or shCTRL-GFP were collected 7 days after mineralization induction. (A) Western blot analysis of the protein expression of odonto/osteogenic markers as indicated. (B) Quantification of western blot results in (A) by normalization to GAPDH. *P<0.05 and **P<0.01 vs. corresponding shCTRL group. GNAI3, guanine and nucleotide binding protein 3; sh[RNA], short hairpin [RNA]; CTRL, control; DSPP, dentin sialophosphoprotein; OCN, osteocalcin; OPN, osteopontin; OSX, osterix; RUNX2, runt-related transcription factor 2.

(P<0.05) 7 days after the mineralization induction of SCAPs, while having no significant effect on p38 phosphorylation (Fig. 5A and B), suggesting that JNK and ERK, but not p38, are the downstream targets of GNAI3. Furthermore, JNK phosphorylation was found to be induced in an apparent time-dependent manner between 0-7 days during the odonto/osteogenic differentiation of SCAPs (Fig. 5C and D), suggesting that JNK proteins may be actively involved in this differentiation process. Additionally, it was found that JNK inhibitor SP600125 and ERK inhibitor U0126 markedly suppressed the proliferation and migration of the SCAPs. Specifically, results indicated that SP600125 and U0126 significantly inhibited cell proliferation after 2-6 days in an apparent time-dependent manner (P<0.01; Fig. 6A and B), as well as cell cycle progression, as evidenced by G1 phase arrest, and S and G2-phase cell reductions (all P<0.05 or <0.01; Fig. 6C-F). In addition, treatment with SP600125 and U0126 caused inhibited migration ability at 12 and 24 h after exposure (P<0.01; Fig. 6G-J). The inhibitory effects of these specific JNK and ERK inhibitors on SCAPs proliferation and migration were consistent with the effects of GNAI3-deficiency in corresponding assays. Taken together, these results suggested that GNAI3 promotes odonto/osteogenic differentiation of SCAPs possibly via JNK and ERK signaling pathways.

Discussion

Tooth root development is a complicated process involving biomineralization, molecular signaling, the development of dental tissue and tooth movement (41,42). Following crown formation, the inner and outer epithelium of the enamel organ extends downwards and forms a double-layered tip known as HERS. In response to the occlusal movement of the teeth, HERS induces the formation and mineralization of the root and determines the tooth morphology (43). GNAI3 has been demonstrated to play a role in regulating various cellular processes including proliferation, cytokinesis, apoptosis, migration and invasion (19,20,44). Causative variants in phospholipase C beta 4, GNAI3 and endothelin 1 during early pharyngeal arch patterning have been identified in ACS, which is characterized by mandibular hypoplasia, suggesting that GNAI3 may be involved in osteogenesis (45). Our previous study demonstrated that GATA4 regulated tooth root development through mediating the expression of GNAI3 (27), which prompted the current investigation into the association of GNAI3 with tooth root development. Since in mice, molar tooth crown and root formation occurs on approximately postnatal day 11 (46), the expression of GNAI3 was detected in the molar teeth of mice on postnatal day 14. It was identified that GNAI3 was markedly upregulated in HERS and

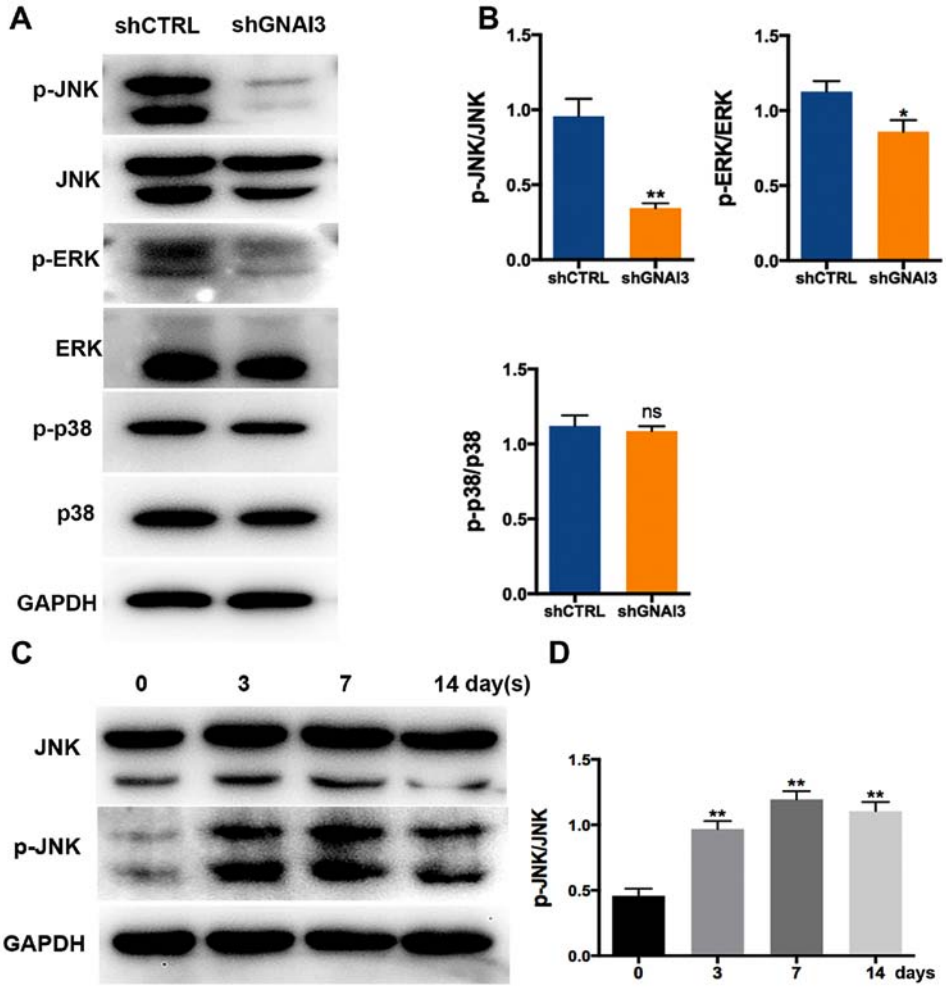

Figure 5. Effect of GNAI3 knockdown on JNK and ERK activation. (A) Western blot analysis of the expression of p-JNK, JNK, p-ERK, ERK, p-p38 and p38. (B) Quantification of western blot results in (A) by normalization to GAPDH. (C) Osteogenic differentiation of stem cells of the apical papilla was induced for the times indicated. The protein levels of p-JNK and JNK were determined by western blotting. (D) Quantification of western blot results in (C). *P<0.05 and **P<0.01 vs. corresponding shCTRL group. GNAI3, guanine and nucleotide binding protein 3; sh[RNA], short hairpin [RNA]; CTRL, control; JNK, c-Jun N-terminal kinase; ERK, extracellular-signal regulated kinase; p-, phosphorylated; ns, not significant.

the surrounding mesenchyme, which serve as two major contributors to root formation, and this was consistent with our previous observation (27), suggesting the possible role of GNAI3 in tooth root development.

SCAPs are located around the open apex of premature tooth root and have odonto/osteogenic potential (47-49). Therefore, we focused on the expression and function of GNAI3 in the odonto/osteogenic differentiation of SCAPs. Consistent with the *in vivo* data, GNAI3 was significantly induced in SCAPs 7 days after mineralization induction. Notably, knockdown of GNAI3 could inhibit the proliferation, migration and odonto/osteogenic differentiation of SCAPs, as key events involved in tooth root development. These results indicated that GNAI3 is required for the mineralization induction of SCAPs. Moreover, knockdown of GNAI3 also suppressed the accumulation of calcium in SCAPs, as evidenced by the decreased ALP activity and ARS staining intensity in GNAI3-deficient SCAPs, suggesting a promotive role of GNAI3 in dentin mineralization.

DMP1, as an acidic non-collagenous protein expressed in a variety of bone and tooth structures, plays a key role during dentin and bone formation (39). DSPP is expressed only in secretory odontoblasts, and regarded as a tooth-specific marker contributing to the formation of dentin (34). RUNX2 is a transcription factor of OSX, and functions in the initial stage of osteogenesis, whereas OPN, OCN and BMP4 have been identified as late stage markers of osteogenesis (35-38). The current study indicated that knockdown of GNAI3 suppressed the expression of these markers at both transcriptional and translational levels, suggesting that GNAI3 plays a universal role in regulating odonto/osteogenic differentiation of SCAPs *in vitro*.

The MAPK signaling pathway is a major orchestrator of complex networks, governing a number of cellular processes and activities including epithelial-to-mesenchymal transition and cell differentiation (24,25,50-55). Recently, it has been established that MAPK signaling may be involved in odonto/osteogenic differentiation of SCAPs (26). However, it remains largely unknown whether GNAI3 functions via MAPK signaling. In the current study, it was found that knockdown of GNAI3 significantly inhibited the phosphorylation of JNK and ERK, two main subfamilies of MAPKs, during SCAPs mineralization. We further determined that specific JNK1/2/3 inhibitor (SP600125) and specific ERK1/2

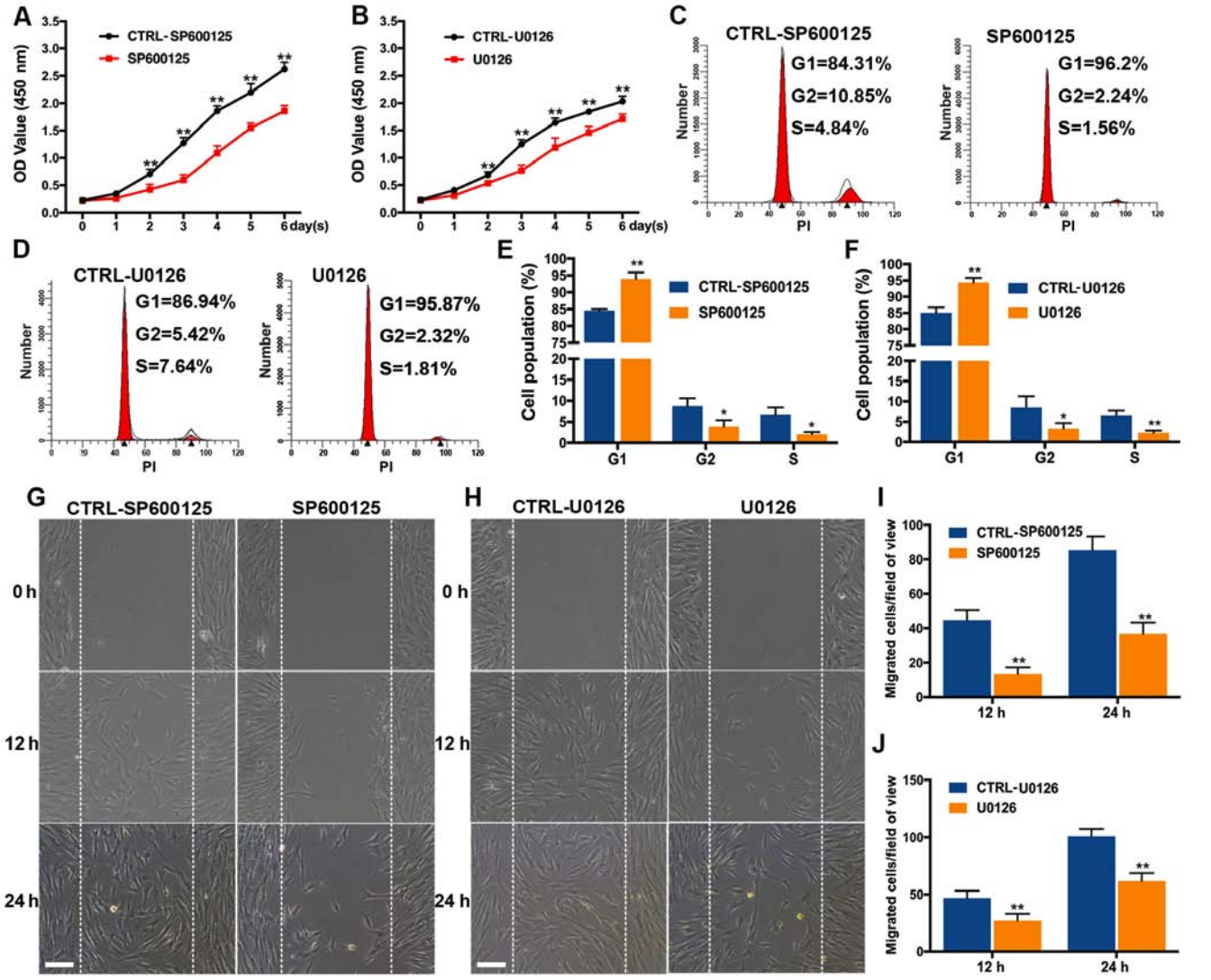

Figure 6. Effect of c-Jun N-terminal kinase inhibitor SP600125 and extracellular-signal regulated kinase inhibitor U0126 on the proliferation and migration of SCAPs. (A and B) Cell Count Kit-8 assay of the time course of SCAPs proliferation following SP600125, U0126 and control treatments. (C-F) Flow cytometry assay of cell cycle progression in SCAPs following the indicated treatments. (G and H) Scratch wound healing assay of SCAPs migration rates at 12 and 24 h of mineralization induction following the indicated treatments. (I and J) Quantification of migration rates in (G and H). Scale bar: 200 μm. *P<0.05 and **P<0.01 vs. corresponding control SCAPs. SCAPs, stem cells of the apical papilla; sh[RNA], short hairpin [RNA]; CTRL, control; OD, optical density; PI, propidium iodide.

inhibitor (U0126) markedly inhibited the proliferation and migration of the SCAPs, consistent with the results that knockdown of GNAI3 inhibited the proliferation and migration of the SCAPs. Thus, it appears that GNAI3 promotes odonto/osteogenic differentiation of SCAPs and tooth root development at least partially through activation of JNK and ERK signaling pathways.

To further verify the role of GNAI3 in odonto/osteogenic differentiation of SCAPs and tooth root development, future studies by our group will perform gain-of-function assays (overexpression of GNAI3) to investigate whether GNAI3 itself is sufficient to induce the odonto/osteogenic differentiation of SCAPs *in vitro*. Furthermore, GNAI3 transgenic mice or SCAPs-specific GNAI3 knockout mice should be used for examination of the *in vivo* role of GNAI3 in tooth root development, which is warranted in further studies.

In conclusion, the present study identified GNAI3 as a novel regulator of odonto/osteogenic differentiation of SCAPs, and provided insight for understanding the mechanisms underlying the regeneration of dentin or other tissues.

Acknowledgements

Not applicable.

Funding

The current study was supported by the National Natural Science Foundation of China (grant nos. 81700942 and 81771029) and the Priority Academic Program Development of Jiangsu Higher Education Institutions (grant no. 2014-037).

Availability of data and materials

The analyzed data sets generated during the study are available from the corresponding author on reasonable request.

Authors' contributions

YZ, LW and JM conceived and designed the study. LY performed the experiments and edited the manuscript. LM and MF analyzed the data. YZ wrote the manuscript. YZ and LY revised the manuscript for intellectual content. SG and DW provided guidance on issues related to the experiments and manuscript writing. All authors read and approved the final manuscript.

Ethics approval and consent to participate

The use of human samples for the study was approved by the Medical Ethics Committee of Stomatological Hospital of Jiangsu Province, Nanjing, China (approval no. PJ2016-038-001). Informed consent was provided by all patients or their next of kin for collection and use of the dental samples. Ethical approval for the animal experimentation (approval no. 2015-03-40) was provided by the Experimental Animal Care and Use Committee of Nanjing Medical University, Nanjing, China.

Patient consent for publication

Written informed consent for publication of related data on patient samples was obtained from all patients or their parents prior to extraction surgery.

Competing interests

The authors declare that they have no competing interests.

References

1. Li Y, Wu Q, Wang Y, Li L, Bu H and Bao J: Senescence of mesenchymal stem cells (Review). Int J Mol Med 39: 775-782, 2017.
2. Garg P, Mazur MM, Buck AC, Wandtke ME, Liu J and Ebraheim NA: Prospective review of mesenchymal stem cells differentiation into osteoblasts. Orthop Surg 9: 13-19, 2017.
3. Tan AR and Hung CT: Concise review: Mesenchymal stem cells for functional cartilage tissue engineering: Taking cues from chondrocyte-based constructs. Stem Cells Transl Med 6: 1295-1303, 2017.
4. Liu GX, Zhu JC, Chen XY, Zhu AZ, Liu CC, Lai Q and Chen ST: Inhibition of adipogenic differentiation of bone marrow mesenchymal stem cells by erythropoietin via activating ERK and P38 MAPK. Genet Mol Res 14: 6968-6977, 2015.
5. Meng X, Sun B, Xue M, Xu P, Hu F and Xiao Z: Comparative analysis of microRNA expression in human mesenchymal stem cells from umbilical cord and cord blood. Genomics 107: 124-131, 2016.
6. Park YJ, Cha S and Park YS: Regenerative applications using tooth derived stem cells in other than tooth regeneration: A literature review. Stem Cells Int 2016: 9305986, 2016.
7. Elahi KC, Klein G, Avci-Adali M, Sievert KD, MacNeil S and Aicher WK: Human mesenchymal stromal cells from different sources diverge in their expression of cell surface proteins and display distinct differentiation patterns. Stem Cells Int 2016: 5646384, 2016.
8. Bakopoulou A and About I: Stem cells of dental origin: Current research trends and key milestones towards clinical application. Stem Cells Int 2016: 4209891, 2016.
9. Ercal P, Pekozer GG and Kose GT: Dental stem cells in bone tissue engineering: Current overview and challenges. Adv Exp Med Biol: Mar 2, 2018 (Epub ahead of print).
10. Yadlapati M, Biguetti C, Cavalla F, Nieves F, Bessey C, Bohluli P, Garlet GP, Letra A, Fakhouri WD and Silva RM: Characterization of a vascular endothelial growth factor-loaded bioresorbable delivery system for pulp regeneration. J Endod 43: 77-83, 2017.
11. Vanacker J, Viswanath A, De Berdt P, Everard A, Cani PD, Bouzin C, Feron O, Diogenes A, Leprince JG and des Rieux A: Hypoxia modulates the differentiation potential of stem cells of the apical papilla. J Endod 40: 1410-1418, 2014.
12. Zou XY, Yang HY, Yu Z, Tan XB, Yan X and Huang GT: Establishment of transgene-free induced pluripotent stem cells reprogrammed from human stem cells of apical papilla for neural differentiation. Stem Cell Res Ther 3: 43, 2012.
13. Prateeptongkum E, Klingelhoffer C and Morsczeck C: The influence of the donor on dental apical papilla stem cell properties. Tissue Cell 47: 382-388, 2015.
14. Guo L, Li J, Qiao X, Yu M, Tang W, Wang H, Guo W and Tian W: Comparison of odontogenic differentiation of human dental follicle cells and human dental papilla cells. PLoS One 8: e62332, 2013.
15. Yu G, Wang J, Lin X, Diao S, Cao Y, Dong R, Wang L, Wang S and Fan Z: Demethylation of SFRP2 by histone demethylase KDM2A regulated osteo-/dentinogenic differentiation of stem cells of the apical papilla. Cell Prolif 49: 330-340, 2016.
16. Chrepa V, Pitcher B, Henry MA and Diogenes A: Survival of the apical papilla and its resident stem cells in a case of advanced pulpal necrosis and apical periodontitis. J Endod 43: 561-567, 2017.
17. Downes GB and Gautam N: The G protein subunit gene families. Genomics 62: 544-552, 1999.
18. Wang Y, Li Y and Shi G: The regulating function of heterotrimeric G proteins in the immune system. Arch Immunol Ther Exp (Warsz) 61: 309-319, 2013.
19. Chen G, Li X, He G, Yu Z, Luo J, He J and Huang Z: Low expression of GNAI3 predicts poor prognosis in patients with HCC. Int J Clin Exp Med 8: 21482-21486, 2015.
20. Hwang IY, Park C, Luong T, Harrison KA, Birnbaumer L and Kehrl JH: The loss of Gnai2 and Gnai3 in B cells eliminates B lymphocyte compartments and leads to a hyper-IgM like syndrome. PLoS One 8: e72596, 2013.
21. Zhang Y, Yao J, Huan L, Lian J, Bao C, Li Y, Ge C, Li J, Yao M, Liang L, *et al*: GNAI3 inhibits tumor cell migration and invasion and is post-transcriptionally regulated by miR-222 in hepatocellular carcinoma. Cancer Lett 356: 978-984, 2015.
22. Kelly P, Moeller BJ, Juneja J, Booden MA, Der CJ, Daaka Y, Dewhirst MW, Fields TA and Casey PJ: The G12 family of heterotrimeric G proteins promotes breast cancer invasion and metastasis. Proc Natl Acad Sci USA 103: 8173-8178, 2006.
23. Rieder MJ, Green GE, Park SS, Stamper BD, Gordon CT, Johnson JM, Cunniff CM, Smith JD, Emery SB, Lyonnet S, *et al*: A human homeotic transformation resulting from mutations in PLCB4 and GNAI3 causes auriculocondylar syndrome. Am J Hum Genet 90: 907-914, 2012.
24. Lu Y, Zhao Q, Liu Y, Zhang L, Li D, Zhu Z, Gan X and Yu H: Vibration loading promotes osteogenic differentiation of bone marrow-derived mesenchymal stem cells via p38 MAPK signaling pathway. J Biomech 71: 67-75, 2018.
25. Li S, Wang J, Han Y, Li X, Liu C, Lv Z, Wang X, Tang X and Wang Z: Carbenoxolone inhibits mechanical stress-induced osteogenic differentiation of mesenchymal stem cells by regulating p38 MAPK phosphorylation. Exp Ther Med 15: 2798-2803, 2018.
26. Diao S, Lin X, Wang L, Dong R, Du J, Yang D and Fan Z: Analysis of gene expression profiles between apical papilla tissues, stem cells from apical papilla and cell sheet to identify the key modulators in MSCs niche. Cell Prolif 50: e12337, 2017.
27. Guo S, Zhang Y, Zhou T, Wang D, Weng Y, Wang L and Ma J: Role of GATA binding protein 4 (GATA4) in the regulation of tooth development via GNAI3. Sci Rep 7: 1534, 2017.
28. Aurrekoetxea M, Irastorza I, Garcia-Gallastegui P, Jimenez-Rojo L, Nakamura T, Yamada Y, Ibarretxe G and Unda FJ: Wnt/beta-catenin regulates the activity of epiprofin/Sp6, SHH, FGF, and BMP to coordinate the stages of odontogenesis. Front Cell Dev Biol 4: 25, 2016.
29. Inoue C, Sobue S, Aoyama Y, Mizutani N, Kawamoto Y, Nishizawa Y, Ichihara M, Abe A, Hayakawa F, Suzuki M, *et al*: BCL2 inhibitor ABT-199 and JNK inhibitor SP600125 exhibit synergistic cytotoxicity against imatinib-resistant Ph+ ALL cells. Biochem Biophys Rep 15: 69-75, 2018.
30. Su X, Wang X, Zhang K, Yang S, Xue Q, Wang P and Liu Q: ERK inhibitor U0126 enhanced SDT-induced cytotoxicity of human leukemia U937 cells. Gen Physiol Biophys 33: 295-309, 2014.

31. Saito MT, Silverio KG, Casati MZ, Sallum EA and Nociti FH Jr: Tooth-derived stem cells: Update and perspectives. World J Stem Cells 7: 399-407, 2015.
32. Zhang W, Zhang X, Ling J, Liu W, Zhang X, Ma J and Zheng J: Proliferation and odontogenic differentiation of BMP2 genetransfected stem cells from human tooth apical papilla: An in vitro study. Int J Mol Med 34: 1004-1012, 2014.
33. Bakopoulou A, Leyhausen G, Volk J, Koidis P and Geurtsen W: Comparative characterization of STRO-1(neg)/CD146(pos) and STRO-1(pos)/CD146(pos) apical papilla stem cells enriched with flow cytometry. Arch Oral Biol 58: 1556-1568, 2013.
34. Iejima D, Sumita Y, Kagami H, Ando Y and Ueda M: Odontoblast marker gene expression is enhanced by a CC-chemokine family protein MIP-3alpha in human mesenchymal stem cells. Arch Oral Biol 52: 924-931, 2007.
35. Nakashima K, Zhou X, Kunkel G, Zhang Z, Deng JM, Behringer RR and de Crombrugghe B: The novel zinc finger-containing transcription factor osterix is required for osteoblast differentiation and bone formation. Cell 108: 17-29, 2002.
36. Huang W, Yang S, Shao J and Li YP: Signaling and transcriptional regulation in osteoblast commitment and differentiation. Front Biosci 12: 3068-3092, 2007.
37. Chen D, Harris MA, Rossini G, Dunstan CR, Dallas SL, Feng JQ, Mundy GR and Harris SE: Bone morphogenetic protein 2 (BMP-2) enhances BMP-3, BMP-4, and bone cell differentiation marker gene expression during the induction of mineralized bone matrix formation in cultures of fetal rat calvarial osteoblasts. Calcif Tissue Int 60: 283-290, 1997.
38. Twine NA, Chen L, Pang CN, Wilkins MR and Kassem M: Identification of differentiation-stage specific markers that define the ex vivo osteoblastic phenotype. Bone 67: 23-32, 2014.
39. Hirst KL, Simmons D, Feng J, Aplin H, Dixon MJ and MacDougall M: Elucidation of the sequence and the genomic organization of the human dentin matrix acidic phosphoprotein 1 (DMP1) gene: Exclusion of the locus from a causative role in the pathogenesis of dentinogenesis imperfecta type II. Genomics 42: 38-45, 1997.
40. Livak KJ and Schmittgen TD: Analysis of relative gene expression data using real-time quantitative PCR and the 2(-Delta Delta C(T)) method. Methods 25: 402-408, 2001.
41. Thesleff I: Epithelial-mesenchymal signalling regulating tooth morphogenesis. J Cell Sci 116: 1647-1648, 2003.
42. Huang Y, Chen N and Miao D: Pyrroloquinoline quinone plays an important role in rescuing Bmi-1(-/-) mice induced developmental disorders of teeth and mandible-anti-oxidant effect of pyrroloquinoline quinone. Am J Transl Res 10: 40-53, 2018.
43. Xiong J, Gronthos S and Bartold PM: Role of the epithelial cell rests of Malassez in the development, maintenance and regeneration of periodontal ligament tissues. Periodontol 2000 63: 217-233, 2013.
44. Rasheed SA, Teo CR, Beillard EJ, Voorhoeve PM and Casey PJ: MicroRNA-182 and microRNA-200a control G-protein subunit alpha-13 (GNA13) expression and cell invasion synergistically in prostate cancer cells. J Biol Chem 288: 7986-7995, 2013.
45. Romanelli Tavares VL, Gordon CT, Zechi-Ceide RM, Kokitsu-Nakata NM, Voisin N, Tan TY, Heggie AA, Vendramini-Pittoli S, Propst EJ, Papsin BC, *et al*: Novel variants in GNAI3 associated with auriculocondylar syndrome strengthen a common dominant negative effect. Eur J Hum Genet 23: 481-485, 2015.
46. Li J, Parada C and Chai Y: Cellular and molecular mechanisms of tooth root development. Development 144: 374-384, 2017.
47. Chueh LH and Huang GT: Immature teeth with periradicular periodontitis or abscess undergoing apexogenesis: A paradigm shift. J Endod 32: 1205-1213, 2006.
48. Sonoyama W, Liu Y, Fang D, Yamaza T, Seo BM, Zhang C, Liu H, Gronthos S, Wang CY, Wang S and Shi S: Mesenchymal stem cell-mediated functional tooth regeneration in swine. PLoS One 1: e79, 2006.
49. Huang GT, Gronthos S and Shi S: Mesenchymal stem cells derived from dental tissues vs. those from other sources: Their biology and role in regenerative medicine. J Dent Res 88: 792-806, 2009.
50. Cao Y, Xia DS, Qi SR, Du J, Ma P, Wang SL and Fan ZP: Epiregulin can promote proliferation of stem cells from the dental apical papilla via MEK/Erk and JNK signalling pathways. Cell Prolif 46: 447-456, 2013.
51. Liao X, Feng B, Zhang D, Liu P, Zhou X, Li R and Ye L: The Sirt6 gene: Does it play a role in tooth development? PLoS One 12: e0174255, 2017.
52. Morris MA, Laverick L, Wei W, Davis AM, O'Neill S, Wood L, Wright J, Dawson CW and Young LS: The EBV-encoded oncoprotein, LMP1, induces an epithelial-to-mesenchymal transition (EMT) via Its CTAR1 domain through integrin-mediated ERK-MAPK signalling. Cancers (Basel) 10: e110, 2018.
53. Yang S, Guo L, Su Y, Wen J, Du J, Li X, Liu Y, Feng J, Xie Y, Bai Y, *et al*: Nitric oxide balances osteoblast and adipocyte lineage differentiation via the JNK/MAPK signaling pathway in periodontal ligament stem cells. Stem Cell Res Ther 9: 118, 2018.
54. Xu P, Wang J, Sun B and Xiao Z: Integrated analysis of miRNA and mRNA expression data identifies multiple miRNAs regulatory networks for the tumorigenesis of colorectal cancer. Gene 659: 44-51, 2018.
55. Chen D, Wang H, Chen J, Li Z, Li S, Hu Z, Huang S, Zhao Y and He X: MicroRNA-129-5p regulates glycolysis and cell proliferation by targeting the glucose transporter SLC2A3 in gastric cancer cells. Front Pharmacol 9: 502, 2018.